tain the permeable solid-state greenhouse underlayer required in the Kirk *et al.* (*22*) model of energy collection and transport for geyser-like plumes. Due to phase transition fracturing, permanent N_2 deposits are highly permeable. The transparent sealing overlayer for the solid-state greenhouse is provided by seasonal condensation if the initial grain size is less than ~1 μm (*20*). Here we assume that enough deposition has occurred on the southern polar cap since the last surface fracturing (according to our model it occurred around A.D. 1920) to produce a transparent layer and that enough time has passed without surface fracturing for initially bright fresh frost to evolve through sintering to a clear N_2 layer. To preserve a low permeability of the greenhouse overlayer (which is a few meters thick) we need to assume again that the approach of the phase boundary from the lower temperature does not disrupt solid N_2.

The transparent layer could be considered as a super-greenhouse overlayer, whereas according to our model the permanent deposits beneath provide multiple fractures in which pressurized N_2 gas can collect and thereby supply geyser vent areas up to 1 km in radius. If this highly pressurized (due to the greenhouse heating) gas finds a vent in a sealing overlayer, it uses the fissures in the permanent deposits to be transported laterally toward the vent.

We hypothesize that geyser vent areas may be created when the impermeable capping overlayer is breached locally in the regions where contamination by CH_4 and CO is higher. Therefore, the phase transition temperature in these local regions is slightly increased in comparison with the less contaminated N_2. These surface areas could be fractured a few years earlier than the ambient N_2 sealing layer, which remains intact until the global surface temperature drops to 35.61 K. This time interval, from our point·of view, will help constrain the lifetime of geyser-like plumes. These speculations are valid only when Triton's surface temperature approaches the phase transition temperature from above.

Recent work by Tryka *et al.* (*23*) suggests that the 2.15-μm absorption band in solid N_2 is sensitive to temperature and to the specific phase of N_2. The predicted variations in phase composition of Triton's permanent polar caps may reveal themselves in changes of the appearance and intensity of the 2.15-μm N_2 absorption band as observed in ground-based spectrophotometry.

REFERENCES AND NOTES

1. D. P. Cruikshank, R. H. Brown, R. N. Clark, *Icarus* **58**, 293 (1984).
2. B. A. Smith *et al.*, *Science* **246**, 1422 (1989).
3. A. W. Harris, in *Uranus and Neptune*, J. Bergstalh, Ed. (NASA CP-2330, Washington, DC, 1984), p. 357.
4. L. Trafton, *Icarus* **58**, 312 (1984).
5. J. R. Spencer, *Geophys. Res. Lett.* **17**, 1769 (1990).
6. J. R. Spencer and J. M. Moore, *Icarus* **99**, 261 (1992).
7. C. J. Hansen and D. A. Paige, *ibid.*, p. 273.
8. R. H. Brown and R. L. Kirk, *JGR Planets*, in press.
9. D. P. Cruikshank *et al.*, abstract presented at conference on Infrared Spectroscopy of Surfaces, San Juan Institute, U.S.A. (1992).
10. R. H. Brown, T. V. Johnson, J. D. Goguen, G. Schubert, M. N. Ross, *Science* **251**, 1465 (1991).
11. R. H. Brown, abstract, *Bull. AAS*, DPS Abstracts, **24**, no. 3 (1992).
12. T. A. Scott, *Phys. Rep.* **27**, 89 (1976).
13. R. A. Jacobson, J. E. Riedel, A. H. Taylor, *Astron. Astrophys.* **247**, 565 (1991).
14. The dimensionless Stefan variable ($S = Q/c\Delta u$) for our problem is ~1.4, so we cannot substitute the problem with just a heat conduction equation, as would apply when $S << 1$. Neither can we take a linear temperature distribution with depth ($S >> 1$), calculated from the temperature gradient at the lower boundary.
15. E. Friedmann, *Proc. 17th Natl. Heat Transfer. Conf.*, 182 (1977).
16. In this method, the temperature field can be found without knowing the interface position at the previous time step, as is necessary in the variational difference method. This advantage is especially noticeable when there are two or more fronts, as in the present case. The enthalpy and the heat conductivity were smoothed with linear polynomials over a very small temperature interval. A fully implicit, time-splitting, finite-difference scheme was applied to solve the smoothed differential problem. The scheme is unconditionally stable, and its approximation order is $O(h_x^2 + h_y^2 + \Delta\tau)$. An iterative method was used to solve the nonlinear discrete system at each time layer. The solution from the previous time step was chosen as an initial approximation for the iterative process. If the process does not converge at either half of the time step, then the time step is bisected.
17. A seventh-order polynomial was used to approximate density, second-order polynomials for the heat resistivity (the inverse of the heat conductivity), and third- and second-order polynomials for the α-N_2 and the β-N_2 heat capacity, respectively.
18. These speculations are valid only for the case when the upper boundary temperature is globally uniform and the media is homogeneous. Recent ground-based spectral observations of Triton's surface by Cruikshank *et al.* (*19*) showed that the content of methane in a mixture with N_2 is much less than 1%. The relative fraction of carbon monoxide to N_2 in an intimate mixture is believed to be 0.1% (*19*). The same relative fraction is derived in (*19*) for carbon dioxide, though it is more likely that carbon dioxide ice is segregated spatially, and can cover ~10% of the surface.
19. D. P. Cruikshank *et al.*, *Science*, **261**, 742 (1993).
20. W. R. Thompson, C. Sagan, *ibid.* **250**, 415 (1990).
21. J. A. Eluszciewicz, *J. Geophys. Res.* **96**, 19217 (1991).
22. R. L. Kirk, R. H. Brown, L. A. Soderblom, *Science* **250**, 424 (1990).
23. K. A. Tryka *et al.*, *Science* **261**, 751 (1993).
24. This research was carried out at the Jet Propulsion Laboratory, California Institute of Technology, Pasadena, California, under a contract with the National Aeronautics and Space Administration.

28 December 1993; accepted 28 April 1993

Spectroscopic Determination of the Phase Composition and Temperature of Nitrogen Ice on Triton

Kimberly A. Tryka, Robert H. Brown, Vincent Anicich,
Dale P. Cruikshank, Tobias C. Owen

Laboratory spectra of the first overtone band (2.1480 micrometers, 4655.4 reciprocal centimeters) of solid nitrogen show additional structure at 2.1618 micrometers (4625.8 reciprocal centimeters) over a limited temperature range. The spectrum of Neptune's satellite Triton shows the nitrogen overtone band as well as the temperature-sensitive component. The temperature dependence of this band may be used in conjunction with ground-based observations of Triton as an independent means of determining the temperature of surface deposits of nitrogen ice. The surface temperature of Triton is found to be $38.0^{+2.0}_{-1.0}$ K, in agreement with previous temperature estimates and measurements. There is no spectral evidence for the presence of α-nitrogen on Triton's surface, indicating that there is less than 10 percent carbon monoxide in solid solution with the nitrogen on the surface.

The presence of molecular nitrogen (N_2) on the surface of Triton was identified from telescopic spectra obtained by Cruikshank *et al.* (*1*) on the basis of a weak absorption band at 2.148 μm, although the physical state of the N_2 was unclear. The presence of N_2 was also deduced from emission lines in Triton's atmospheric spectrum seen by the ultraviolet (UV) spectrometer experiment on Voyager 2 during its 1989 flyby (*2*). Thermal measurements made by the Voyager infrared spectrometer indicated a surface temperature of 38^{+3}_{-4} K (*3*), and a surface pressure of 14 μbar was derived from measurements by the UV spectrometer (*2*). As the triple-point temperature of N_2 is

K. A. Tryka, Division of Geological and Planetary Sciences, California Institute of Technology, Pasadena, CA 91125.
R. H. Brown and V. Anicich, Jet Propulsion Laboratory, MS 183-501, California Institute of Technology, Pasadena, CA 91109.
D. P. Cruikshank, National Aeronautics and Space Administration, Ames Research Center, MS 245-6, Moffett Field, CA 94035.
T. C. Owen, Institute for Astronomy, University of Hawaii, Honolulu, HI 96822.

63.15 K (*4*), the Voyager measurements showed that N_2 is present in Triton's atmosphere and exists on the surface as a solid. The close correspondence of the basal temperature and pressure of Triton's atmosphere to that of vapor-pressure equilibrium [14 μbar at 37.5 K (*5*)] also suggests that the gas is in vapor-pressure equilibrium with the surface ice.

Since the Voyager 2 encounter with Triton, new infrared spectrometers have made possible significant advances in our understanding of the composition, physical state, and distribution of the major components of Triton's surface. In this report we analyze recent ground-based observations of Triton that have yielded spectra of higher resolution than had been previously available and that show additional structure near the N_2 band center, including an unidentified absorption at 2.162 μm (*6*). From these ground-based data and high-precision laboratory measurements of the transmission spectrum of N_2 ice reported here, both the temperature and the phase of N_2 ice on Triton can be determined. In addition, the 2.162-μm absorption feature in Triton's spectrum can now be identified.

At pressures and temperatures relevant to Triton, solid N_2 exists in two distinct phases. The β phase is a low-density phase with a hexagonal crystal structure that exists above 35.6 K (at zero pressure). The α phase is a high-density phase with a cubic structure that exists below 35.6 K at zero pressure (*4*). A third known phase of solid N_2, the γ phase, exists only at high pressures and is not of interest here. The temperature of the α-β transition is strikingly close to the measured surface temperature of Triton. In addition, seasonal volatile transport on Triton causes large fluctuations in Triton's globally averaged temperature on time scales of decades to centuries (*7–9*). The temperatures are such that Triton's surface ices are continuously cycled through the α-β phase transition (*10*). Therefore, on the basis of thermodynamic arguments alone, it has not been possible to rule out the presence of either the α or the β phase of N_2 ice on Triton.

Molecular nitrogen exhibits a sparse spectrum of near-infrared absorptions caused by an induced-dipole transition (*4*), and it is expected that changes in the proximity of neighboring N_2 molecules brought about by changes in temperature and crystal structure will have measurable effects on the near-infrared transmission spectrum of N_2 ice.

Preliminary laboratory work indeed suggests that the shape and strength of both the fundamental vibrational transition at 4.2942 μm (2328.7 cm^{-1}) and its first overtone at 2.1480 μm change substantially as N_2 goes through the α-β phase transition (*11*). This work led us to conclude that better quality laboratory measurements combined with higher precision spectra of Triton might lead to an identification of the specific phase of N_2 on Triton.

Transmission spectra of solid N_2 were measured at the Extraterrestrial Ice Facility at the Jet Propulsion Laboratory (*12, 13*). Similar measurements have recently been made by Grundy *et al.* (*14*).

To form an optically clear sample of β-N_2, we slowly cooled liquid N_2 through the triple point as suggested by previous experimenters (*4*). When this method is used, a typical sample freezes optically clear although a small void space in the center of the sample forms as the N_2 contracts during cooling. To minimize the well-documented cracking that occurs in samples of solid N_2 as they are cooled through the α-β phase transition (*4*), we cooled our samples at a rate of 0.02 K per minute. As a result, the N_2 ice remained clear to a temperature of ~45 K, where the sample began to show some limited cracking. After passing through the α-β phase transition, samples became extensively cracked on length scales of several tens of micrometers and had a translucent, white appearance. Although the signal transmitted through the cracked sample was considerably less (by a factor of ≈25) than the signal through the clear sample, it was adequate for spectral measurements.

We divided each measurement of the transmission of a given sample by a measurement of the transmission of the empty cell to remove the spectrometer response function. Because a typical sample was left in the cell for a period of days, measurements of the empty cell transmission were taken both before the sample was formed and after it was evaporated.

To facilitate direct comparisons of our laboratory data with observations of Triton, several steps were taken. First, the transmittance data were normalized in the continuum to correct for void space and scattering in the sample and to provide a common reference level for the separate measurements (*15*). The normalized transmittances for three different temperatures are shown in Fig. 1, A, B, and C. A second band, seen at 2.16 μm in Fig. 1B, appears only over a limited range of temperatures (41 K to just above the phase-transition temperature). We derived absorption coefficients from the normalized transmittance data by converting transmittance to absorbance and then dividing the absorbance by the cell length. Because the resolution of the laboratory data was not the same as that of the observational data, the laboratory data were degraded to the resolution of the observational data. This was accomplished by convolving the laboratory data with a Gaussian of the appropriate half-width and amplitude. The resulting absorption coefficient spectrum was used to model the radiance coefficient (*16*) of particulate N_2 ice, for comparison with the Triton spectrum. The radiance coefficient is the ratio of the reflectance of a surface to the reflectance of a Lambert surface identically illuminated. To calculate this quantity, we used an index of refraction of 1.2 (*17*). Isotropic scattering was assumed, along with surface-normal illumination and reflection. Parameters specifying the opposition effect and macroscopic roughness of a surface were ignored.

The remaining two parameters to be specified for the model fitting process are single-scattering albedo and particle size. In the case of an optically thin medium, single-scattering albedo is a function of the absorption coefficient and particle size (*16, 18*). The absorption coefficient spectrum as a function of temperature is determined by our laboratory measurements. The effect of

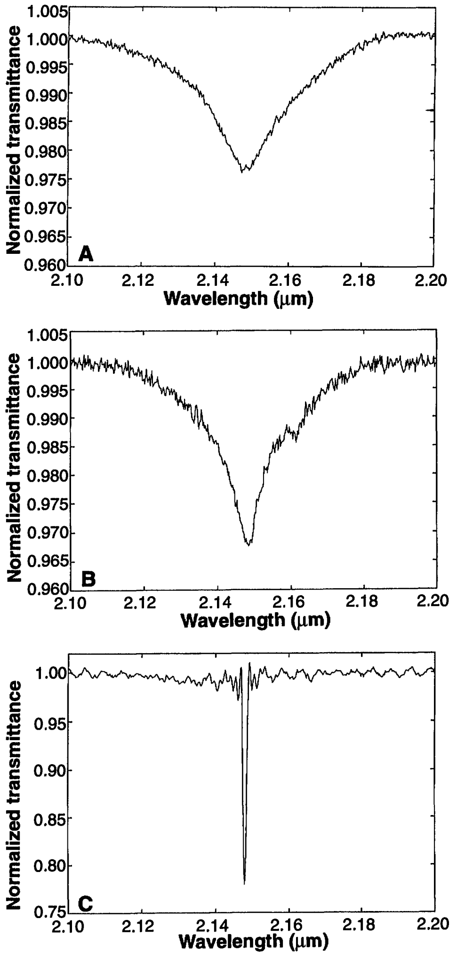

Fig. 1. Normalized transmittance spectra of solid N_2, 2.10 to 2.20 μm, at temperatures of (**A**) 49.4 K, (**B**) 39.1 K, and (**C**) 35.5 K. Note the presence of a second band at 2.16 μm in the spectrum at 39.1 K that does not appear in the other spectra.

increasing particle size, for a given set of absorption coefficients, is to deepen and broaden the band being modeled. Representative results of the model fits are shown by the lines in Fig. 2, A and B.

In both Fig. 2A and Fig. 2B the discrete points are observations of Triton taken in May 1992 (*1*), with the bars representing the point-to-point scatter of the data. The data are normalized to 1.0 in the continuum, and the 2.2-μm CH_4 absorption band was removed to isolate the N_2 band. We removed the CH_4 absorption by modeling it as a combination of two Gaussians and dividing the spectrum by these Gaussians. Removal of the CH_4 band does not affect the data shortward of 2.175 μm; it merely corrects the downturn of the long-wavelength portion of the N_2 band, which occurs because it is superposed on the CH_4 band.

Figure 2A shows the four temperatures that best match the observational data, as determined by least squares fits. These models match the width and intensity of the broad 2.15-μm band and display a band at 2.16 μm, although it is weaker than that seen in the observational data. One explanation of this mismatch is possible contamination of N_2. It is unlikely that N_2 is present as an isolated substance on the surface of Triton; rather, N_2 will be contaminated by small amounts of volatile species such as CO and CH_4 (*6*). If that is the case, the presence of these other species may influence the spectral signature of N_2. To our knowledge, absorption coefficients for these mixtures have not been measured; thus, we assume, for this discussion, that the spectral line in question is produced by pure N_2.

The best fit is for a temperature of 38.9 K and a particle diameter of 0.43 cm. The next best fits correspond to temperature-size combinations of 37.8 K and 0.41 cm, 37.3 K and 0.42 cm, and 39.4 K and 0.45 cm. The χ^2 of the best fit is 6.67×10^{-3}, and the next best fits give a χ^2 in the range 7.20×10^{-3} to 8.00×10^{-3}. Other models had a χ^2 significantly outside the range quoted above ($>8.6 \times 10^{-3}$). We therefore conclude that the range $38.0^{+2.0}_{-1.0}$ K encompasses the temperature of N_2 ice on Triton. These limits are not based on statistical arguments; they only represent the point at which the χ^2 indicates a significantly worse fit. The quoted range of temperatures includes the point at which the equilibrium vapor pressure of N_2 is 14 μbar. As such, our result supports the assumption that N_2 gas in the lower atmosphere of Triton is in vapor-pressure equilibrium with the solid on the surface.

Figure 2B demonstrates that N_2 ice at temperatures outside this range does not display the spectral line shape seen in the Triton spectrum. The two models shown are for temperatures of 49.4 and 35.7 K, with a particle size of 0.45 cm. The model spectrum for the higher temperature sample has a width and depth similar to those of the band on Triton but lacks the additional structure at 2.16 μm. The model for the lower temperature sample shows a deep, narrow absorption characteristic of α-N_2, which is not seen in the Triton spectrum. Thus, there is no spectral evidence for the presence of α-N_2 on Triton.

It is known that N_2 and CO are soluble in all proportions and that the addition of CO in N_2 has the effect of raising the α-β transition temperature (*4*) as well as lowering the vapor pressure. This, along with the lack of a spectral signature of α-N_2 in the Triton spectrum, can be used to place an upper limit on the amount of CO that might be present in solid solution with N_2 on Triton's surface. If the N_2 temperature is no higher than 40 K, then the phase diagram of the CO-N_2 solid solution series shows that there must be less than ≈10% CO in solution with the N_2; otherwise, Triton's spectrum would display the deep, narrow signature of α-N_2. This upper limit is far higher than the 0.1% abundance of CO inferred by Cruikshank *et al.* (*6*), which was based on model fits to the 2.35-μm band in Triton's spectrum.

Owen *et al.* (*19*) identifies N_2 in the spectrum of Pluto. If spectra of higher resolution and precision can be obtained, one can estimate the temperature of N_2 on Pluto by using the technique that we apply here for Triton. If N_2 is the largest component of the atmosphere and surface of Pluto, its temperature could be very close to the actual surface temperature of the planet.

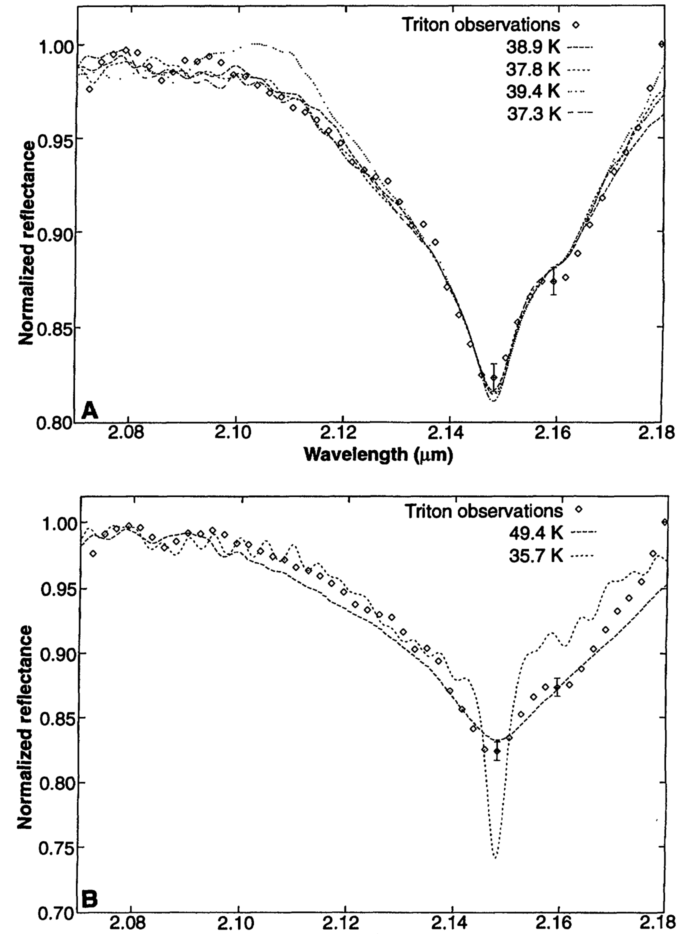

Fig. 2. The infrared spectrum of Triton (+), 2.07 to 2.18 μm, and models of the spectrum from transmission measurements of solid N_2 as described in the text. The Triton observations are normalized to 1.0 in the continuum, and the modeled spectra have been normalized so that the average value in the range 2.07 to 2.10 μm matches the average continuum value of the observational data in the same region. The error bars represent the point-to-point scatter in the observational data. (**A**) The four models shown are for temperature–particle size combinations of 38.9 K and 0.43 cm, 37.8 K and 0.41 cm, 37.3 K and 0.42 cm, and 39.4 K and 0.45 cm. (**B**) Models for temperatures of 49.4 and 35.7 K and a particle size of 0.45 cm.

REFERENCES AND NOTES

1. D. P. Cruikshank, R. H. Brown, R. N. Clark, *Icarus* **58**, 293 (1984).
2. A. L. Broadfoot *et al.*, *Science* **246**, 1459 (1989).
3. B. Conrath *et al.*, *ibid.*, p. 1454.
4. T. A. Scott, *Phys. Rep.* **27**, 89 (1976).
5. G. N. Brown, Jr., and W. T. Ziegler, *Adv. Cryog. Eng.* **25**, 662 (1980).
6. D. P. Cruikshank *et al.*, *Science* **261**, 742 (1993).
7. J. R. Spencer, *Geophys. Res. Lett.* **17**, 1769 (1990).
8. R. H. Brown, *Bull. Am. Astron. Soc.* **24**, 966 (1992).
9. ——— and R. L. Kirk, in preparation.
10. N. S. Duxbury and R. H. Brown, *Science* **261**, 748 (1993).
11. J. R. Green, R. H. Brown, D. P. Cruikshank, V. Anicich, *Bull. Am. Astron. Soc.* **23**, 1208 (1991).

12. Our data were taken using a Fourier transform spectrometer. The spectrometer was fitted with a CaF_2 beam splitter, a tungsten source, and an InSb detector. Data were taken between 1 and 5 μm (2000 and 10000 cm^{-1}) and spanned a temperature range of 35 to 60 K. The spectral resolution was 5×10^{-4} μm at 2.15 μm (1 cm^{-1}). Our integration period was 4 min. Backgrounds were taken with the same integration period. The N_2 from which our samples were formed is of research quality (99.9995% pure). A sample of solid N_2 was held in a cell attached to a cold finger, cooled by a closed-cycle He refrigerator. The temperature controller used in the experiments is capable of millikelvin resolution and is able to hold a sample at a constant temperature (± 0.02 K) for several hours.
13. K. A. Tryka, R. H. Brown, V. Anicich, in preparation.
14. W. M. Grundy, B. Schmitt, E. Quirico, in preparation.
15. The continuum absorption of N_2 is <1% in this wavelength region, which makes an accurate measurement of this quantity extremely difficult. Because it is the relative depths of the bands that are the important quantity, we chose to normalize the transmittance data to 1.0 in the continuum, providing a common reference level from which to quote results.
16. B. Hapke, *J. Geophys. Res.* **86**, 3039 (1981).
17. R. C. Weast, Ed., *CRC Handbook of Chemistry and Physics* (CRC Press, Boca Raton, FL, 1980). Because there is no measurement of the index of refraction of solid N_2 in the literature, we used the index of refraction of liquid N_2 as given in this reference.
18. R. N. Clark and T. L. Roush, *J. Geophys. Res.* **89**, 6329 (1984).
19. T. C. Owen *et al.*, *Science* **261**, 745 (1993).
20. We thank two anonymous referees for useful comments. This is contribution 5281 of the Division of Geological and Planetary Sciences, California Institute of Technology.

2 March 1993; accepted 3 June 1993

Requirement of Salicylic Acid for the Induction of Systemic Acquired Resistance

Thomas Gaffney, Leslie Friedrich, Bernard Vernooij,
David Negrotto, Gordon Nye, Scott Uknes, Eric Ward,
Helmut Kessmann, John Ryals*

It has been proposed that salicylic acid acts as an endogenous signal responsible for inducing systemic acquired resistance in plants. The contribution of salicylic acid to systemic acquired resistance was investigated in transgenic tobacco plants harboring a bacterial gene encoding salicylate hydroxylase, which converts salicylic acid to catechol. Transgenic plants that express salicylate hydroxylase accumulated little or no salicylic acid and were defective in their ability to induce acquired resistance against tobacco mosaic virus. Thus, salicylic acid is essential for the development of systemic acquired resistance in tobacco.

Infection of plants with a necrotizing pathogen can enhance the plants' resistance to subsequent infections by a variety of bacterial, fungal, and viral pathogens (*1*). This physiological immunity, also known as systemic acquired resistance (SAR), is an integral and important component of a plant's defense against disease. Among the more interesting aspects of acquired resistance are that the resistance extends to plant tissues distant from the initial infection site, persists for weeks to months after the initial infection, and protects against a broad spectrum of plant pathogens (*1*). These characteristics make SAR a promising target for the discovery of therapeutics to control plant diseases (*2*).

In tobacco, cucumber, and *Arabidopsis*, SAR is strongly correlated with the coordinate expression of a set of genes (SAR genes) encoding proteins that include the "pathogenesis-related" (PR) proteins (*3–5*). How these proteins contribute to resistance is unknown, although several function as antibiotics when tested against plant pathogens in vitro (*6*). In addition, one of the SAR genes, PR-1a, confers tolerance to two different oomycete pathogens when it is expressed in transgenic tobacco (*7*). Thus, these proteins may be causally involved in maintaining the disease-resistant state.

Although the phenomenon of SAR has been known for almost a century and has been described in many reports (*1*), the way in which the resistant state is induced is still poorly understood. After pathogen infection, but before the onset of resistance, salicylic acid (SA) accumulates in the phloem of cucumber and tobacco plants (*8, 9*). The exogenous application of SA to tobacco leaves mimics the pathogen-induced SAR response by inducing the same set of SAR genes, as well as resistance, in treated tissue (*3, 4–10*). Consequently, it has been postulated that SA serves as an endogenous signal molecule required for SAR induction (*3, 8, 9*).

If an increase in endogenous SA is required to establish acquired resistance, then a barrier to SA accumulation should block the development of SAR. Salicylate hydroxylase (E.C. 1.14.13.1), encoded by the *nah*G gene of *Pseudomonas putida*, is a flavoprotein that catalyzes the decarboxylative hydroxylation of salicylate, converting it to catechol (Fig. 1) (*11*). A DNA fragment containing the *nah*G coding sequence from *P. putida* PpG7 (*12*) was subcloned from pSR20 (*13*) into an expression vector in which transcription is controlled by the enhanced 35S cauliflower mosaic virus promoter and terminated by the *tml* 3′ terminator (*13*). We transformed the final construct into tobacco using *Agrobacterium* (*13*). Independently transformed plants were screened for *nah*G mRNA accumulation, and several transformants were selected for further analysis. We allowed these plants to self-pollinate for two generations and then identified lines homozygous for the selectable marker by screening for antibiotic resistance.

To determine the effect of *nah*G gene expression on the accumulation of SA, we inoculated three lower leaves of plants from each of the lines with tobacco mosaic virus (TMV). After 7 days, when lesions had formed on the infected leaves, we harvested leaf tissue and assayed for *nah*G mRNA (*14*), salicylate hydroxylase protein (*15*), and SA (*16*). The nontransformed control line infected by TMV accumulated ~6000 ng of SA per gram of tissue, representing a 185-fold increase relative to plants treated with medium but no virus (Fig. 2), a result consistent with previous findings (*8, 17,*

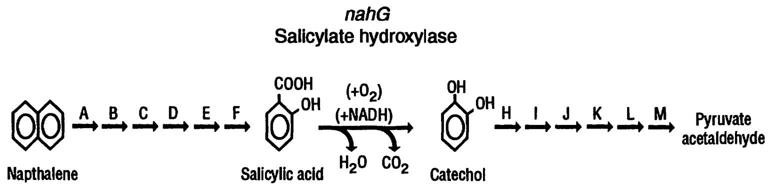

Fig. 1. Function of *nahG*. Biochemical degradation of naphthalene by *P. putida* strain PpG7 occurs in 13 steps encoded by the bacterial *nah* genes (*12*). The letters A to M represent the enzymes encoded by the genes *nahA* to *nahM*. The *nahG* gene encodes salicylate hydroxylase that uses NADH (reduced form of nicotinamide adenine dinucleotide) as a cofactor to decarboxylate and hydroxylate SA to catechol.

T. Gaffney, L. Friedrich, B. Vernooij, D. Negrotto, G. Nye, S. Uknes, E. Ward, J. Ryals, Agricultural Biotechnology Research Unit, Ciba-Geigy Corporation, Post Office Box 12257, Research Triangle Park, NC 27709.
H. Kessmann, Plant Protection, Ciba-Geigy Limited, CH4002 Basel, Switzerland.

*To whom correspondence should be addressed.